Large-Eddy Simulation for Turbulent Nature of Flow and Pressure Fields over Urban Building Arrays

C. Hirose*, A. Hagishima, N. Ikegaya, and J. Tanimoto

Interdisciplinary Graduate School of Engineering Sciences, Kyushu University, Kasuga, Fukuoka, 816-8580, Japan

ABSTRACT

Large-eddy simulation is used to investigate velocity and pressure fields over arrays of urban buildings, represented by regular cubes. The mean distributions of wall pressure are dominated by the robust flow structures around the cube arrays. On the other hands, the results demonstrate the significant difference in wall pressure distribution between instantaneous snapshots and the mean values. A sequence of snapshots of the instantaneous flow and pressure fields indicates that the discrepancy from the mean fields is derived from the unsteady, three-dimensional turbulent structure of airflow around the cubes. The findings suggest that the transient nature of the turbulence above the urban canopy strongly influences wind-induced natural ventilation in urban buildings.

KEYWORDS

Large-eddy simulation, Natural ventilation, Wind pressure coefficient

INTRODUCTION

Wind-induced natural ventilation through a building can contribute to reducing the consumption of energy for air-conditioning, to lowering greenhouse gas emissions, as well as the improvement of thermal comfort and indoor air quality. Since natural ventilation is driven by the pressure difference between two walls with openings, the accurate estimation of the distribution of wall pressure throughout a building is essential to designing healthy, comfortable, and sustainable buildings.

In the field of wind engineering, the flow structure around a bluff body and the pressure acting on its surfaces have been long-standing issues, and knowledge of these issues has been successfully applied to building design for safety—in terms of wind resistance—as well as natural ventilation (e.g., Marshall, 1975). Several studies have shown the obvious effects of the unsteady dynamics of the turbulent flow on wind-driven ventilation (e.g., Haghighat et al., 1991; Jiang et al., 2001).

* email address: 2es13171m@s.kyushu-u.ac.jp

Considering recent work on the turbulent organized structure that developed over urban building arrays in an urban climatology community (e.g., Kanda, 2006), it would be interesting to determine how the turbulence at the urban boundary affects wind-driven ventilation in an urban building. Despite numerous previous studies on wind-induced natural ventilation, there remain few detailed studies focusing on the instantaneous behavior of wall pressure associated with the unsteady turbulent flow within the urban canopy layer.

We therefore conducted large-eddy simulation (LES) in order to investigate the mean and temporal features and relationships of the velocity and pressure fields over arrays of urban buildings.

RESEARCH METHODS

The airflow over two types of uniform building arrays are investigated using the LES: square array (hereafter SQ) and staggered array (hereafter ST). Fig. 1 shows schematics of the simulation domains. The building models are cubes of 24 mm (hereafter H) on each side and the plan area index is 0.25 in both cases. Periodic boundary conditions are imposed in the streamwise and lateral directions, a free-slip boundary condition is applied at the top of the domain, and the bottom wall and all cube surfaces are set as the no-slip boundary. An isotropic and uniform Cartesian grid was used, with grid size of H/16. The initial running duration from t = 0 to 100 s and the averaging time from t = 100 to 160 s satisfy the initial duration: 200T and averaging time for statistical convergence: 400T, where $T = H/u^*$ suggested by Coceal et al. (2006).

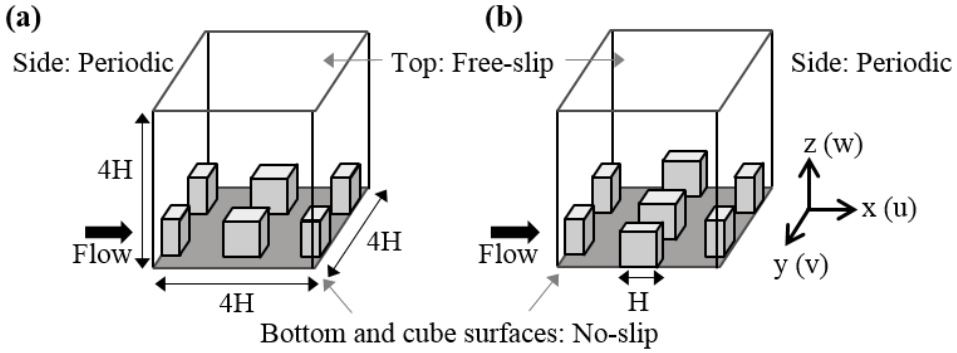

Fig. 1 Schematics of computational domain. (a) Square array: SQ (b) Staggered array: ST

The numerical simulation utilizes OpenFOAM open-source CFD software. The sub-grid scale (SGS) model of the LES is a standard Smagorinsky model and the Smagorinsky constant is set as 0.168. The flow is driven by the pressure gradient, so as to maintain a streamwise bulk velocity of 1.5m/s.

The simulated mean flow statistics were validated by comparison the DNS data reported by Coceal et al. (2006), which confirmed that the calculation accuracy is acceptable for the present purposes.

MEAN CHARACTERISTICS OF WALL PRESSURE

3.1. Spatially averaged wall pressure

The wind pressure coefficient C_p defined by the wind speed at vertical height z = 2H is derived from equation (1):

$$C_{p(2H)} = \frac{P_f - P_b}{1/2 \rho U_{(2H)}^2}, \quad (1)$$

where P_f and P_b are the pressure on the front and back faces of the wall, respectively. The spatially averaged values of C_p for a block in a computational domain of both arrays are shown in Fig. 2 with the experimental results for various packing densities obtained by Zaki et al. (2012). Our estimation of C_p in ST (λ_p=25%) is much larger than that in SQ, which is consistent with the experimental results.

Figs. 3(a) and 3(b) show the vertical profiles of C_p normalized by the face-averaged values denoted by $\langle C_{p(2H)} \rangle$, and the normalized pressure acting on front and back faces, respectively. In Fig. 3(a), the two arrays show contrasting tendencies. For example, the maximum C_p in SQ is observed at the very top of the cube and decreases markedly with height; in contrast, ST shows relatively small deviation. Such clear difference in C_p is caused by the differing pressure distributions on the front wall of the two layouts.

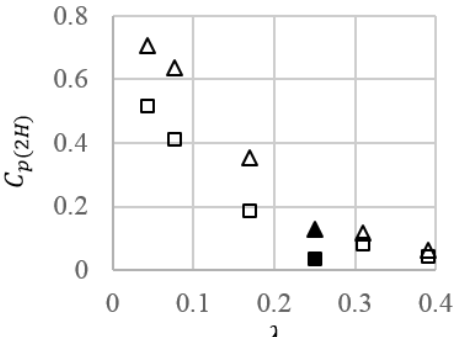

Fig. 2 Wind pressure coefficient: C_p defined by mean velocity at z=2H for different packing densities. ■: SQ. ▲: ST. □: SQ1 and △:ST1 (Zaki et al., 2012).

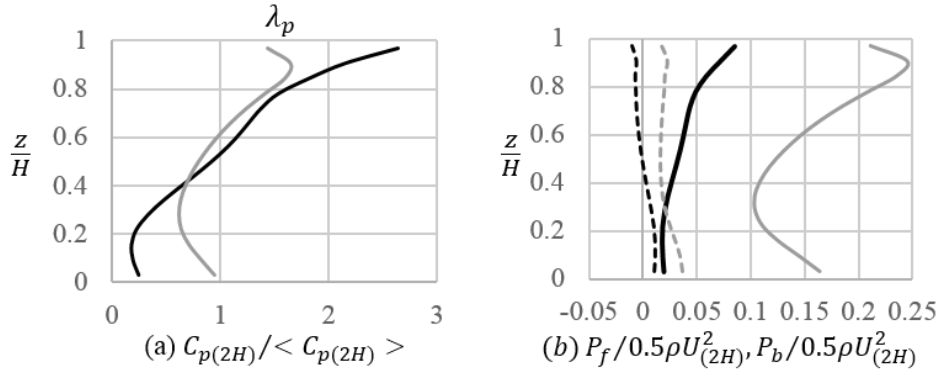

Fig. 3 Vertical profiles of (a) normalized wind pressure coefficient (Black line: SQ. Gray line: ST.) and (b) normalized pressure acting on cubes (Solid lines: $P_f/0.5\rho U_{(2H)}^2$. Dotted lines: $P_b/0.5\rho U_{(2H)}^2$.).

3.2. Spatial distribution and fluctuation of wind pressure

The wall surface distributions of wind pressure coefficient and the fluctuating wind

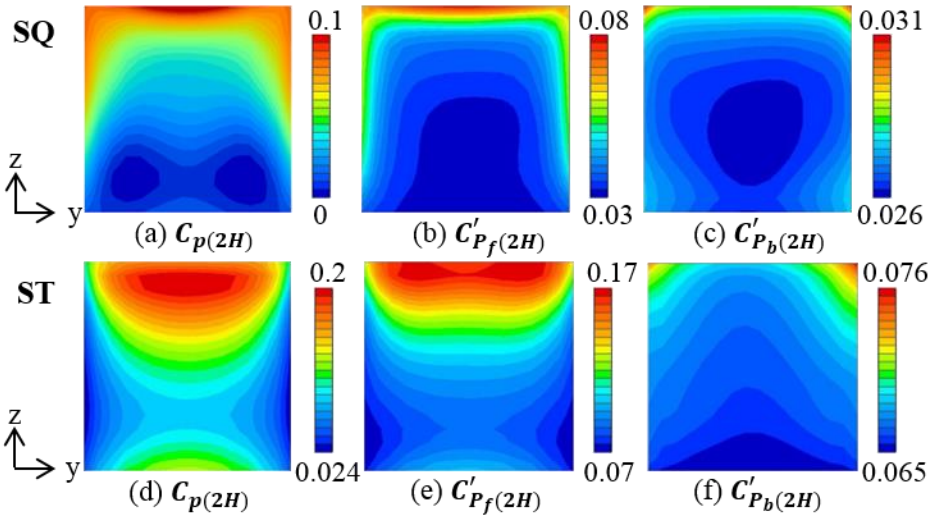

Fig. 4 Surface distributions of (a) wind pressure coefficient and fluctuating wind pressure coefficient on (b) front and (c) back surface defined by the reference velocity at z=2H for SQ. (d), (e) and (f) are the same as (a), (b) and (c), but for ST.

pressure coefficient C'_p defined by the wind speed at z=2H are expressed by equation (2) and shown in Fig. 4,

$$C'_{p(2H)} = \frac{\sigma_p}{1/2 \rho U^2_{(2H)}}, \quad (2)$$

where σ_p is the standard deviation of wall pressure.

Comparison of Figs. 4(a) and 4(d) reveals that C_p for SQ is relatively large at the outer edge of the wall and negative peaks are observed symmetrically at the lower half of the wall, whereas C_p for ST is larger at the upper end line, which spreads downward to half the height of the cube. Considering the mean flow structures presented by Coceal et al. (2006), it seems that the distributions of high-pressure areas on the cube are closely related to the regions exposed to strong wind, such as the skimming flow with shorter interval of blocks in the streamwise direction in SQ, and the downward-wind significantly penetrating the canopy layer in ST.

Furthermore, such flow characteristics result in considerable fluctuation in the front wall pressure for each array, as shown in Figs. 4 (b) and 4(e). On the other hand, C'_{P_b} for each array is much smaller compared to corresponding C'_{P_f} in geometry. This might be caused by the weak velocity and fluctuation behind the cube, especially where the counter-rotating vortex pair is constantly observed for both arrays, as is widely reported (e.g., Coceal et al. 2006).

INSTANTANEOUS DISTRIBUTION OF VELOCITY AND PRESSURE FIELDS

Figs. 6 and 7 give a sequence of snapshots of the instantaneous flow fields around the cube and the pressure acting on the front and back walls, as illustrated in Fig. 5. The figures show that the unsteady and three-dimensional structure of turbulence within and

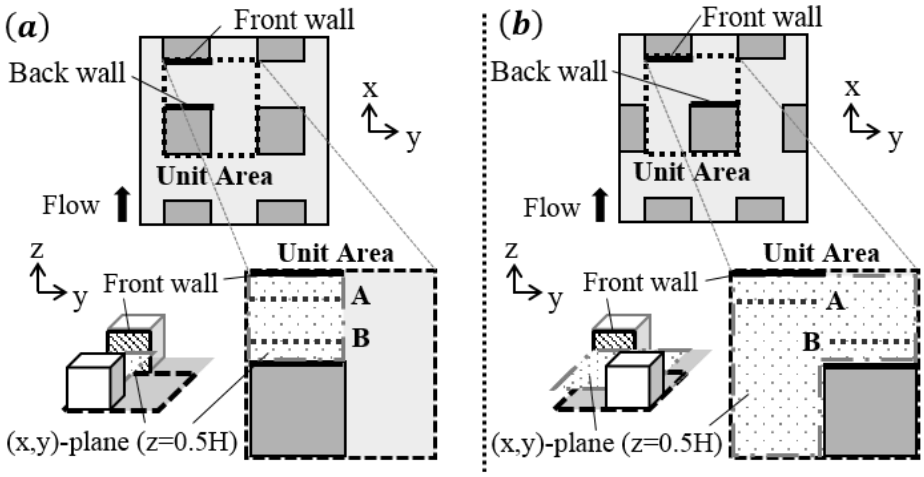

Fig. 5 Schematics of data sampling positions for (a) SQ and (b) ST. The snapshots of wall pressure distribution are extracted at front and back walls. The snapshots of flow structures are obtained at (x, y)-planes at the height of 1.5H (in unit area), 1H, 0.5H, and 0.16H, and at (y, z)-planes: A and B separated by 0.22H from front and back walls, respectively.

above the canopy layer dominates the distributions of instantaneous wall pressure, which are entirely different from those of the mean pressure shown in Fig. 4.

As for SQ, the high- and low-speed streaks elongated in the streamwise direction are depicted at the height of 1.5H in Fig. 6(a). Within the canopy layer, the high-speed flow penetrating the cavity (i.e., the region between successive cubes within the rows) from the unobstructed channel region parallel to the mean wind leads to reverse or recirculating flow, as presented in Figs. 6(c) and 6(d). Comparison between Figs. 6(c), 6(d), and Fig. 6(e) shows that the high-pressure and low-pressure areas on walls are consistent with the collision point and the separation point of strong wind, respectively.

As for ST, the unsteady penetration of the high-speed streak can be observed in Figs. 7(a) and 7(b), as seen for SQ. However, the tendency in ST is more obvious than that in SQ, although the present comparison only includes data for a limited period. As can be seen in Figs. 7(b) and 7(e), the wider ranges of higher-pressure regions are formed due to the collision of faster flow above the canopy layer. Furthermore, the high-speed flow that is generated by the convergence of diverged flows due to the presence of the cubes in the upstream region (e.g., Figs. 7(c-4)) impinges upon the entire front wall, such that strong downward flow as well as dispersed flow in the lateral direction are generated in front of the cube. As a result of these instantaneous flow structures, the high-pressure area on the front wall tends to spread deep into the canopy layer, and a negative-pressure region arises instantaneously, as shown in Fig. 7(e-2).

For the pressure distributions on the back wall shown in Figs. 6(g) and 7(g), the ranges of the temporal changes exceed those of the instantaneous distributions for both arrays. This might be a result of the weak and almost steady flow structures behind the cube, as can be seen in Figs. 6(h) and 7(h).

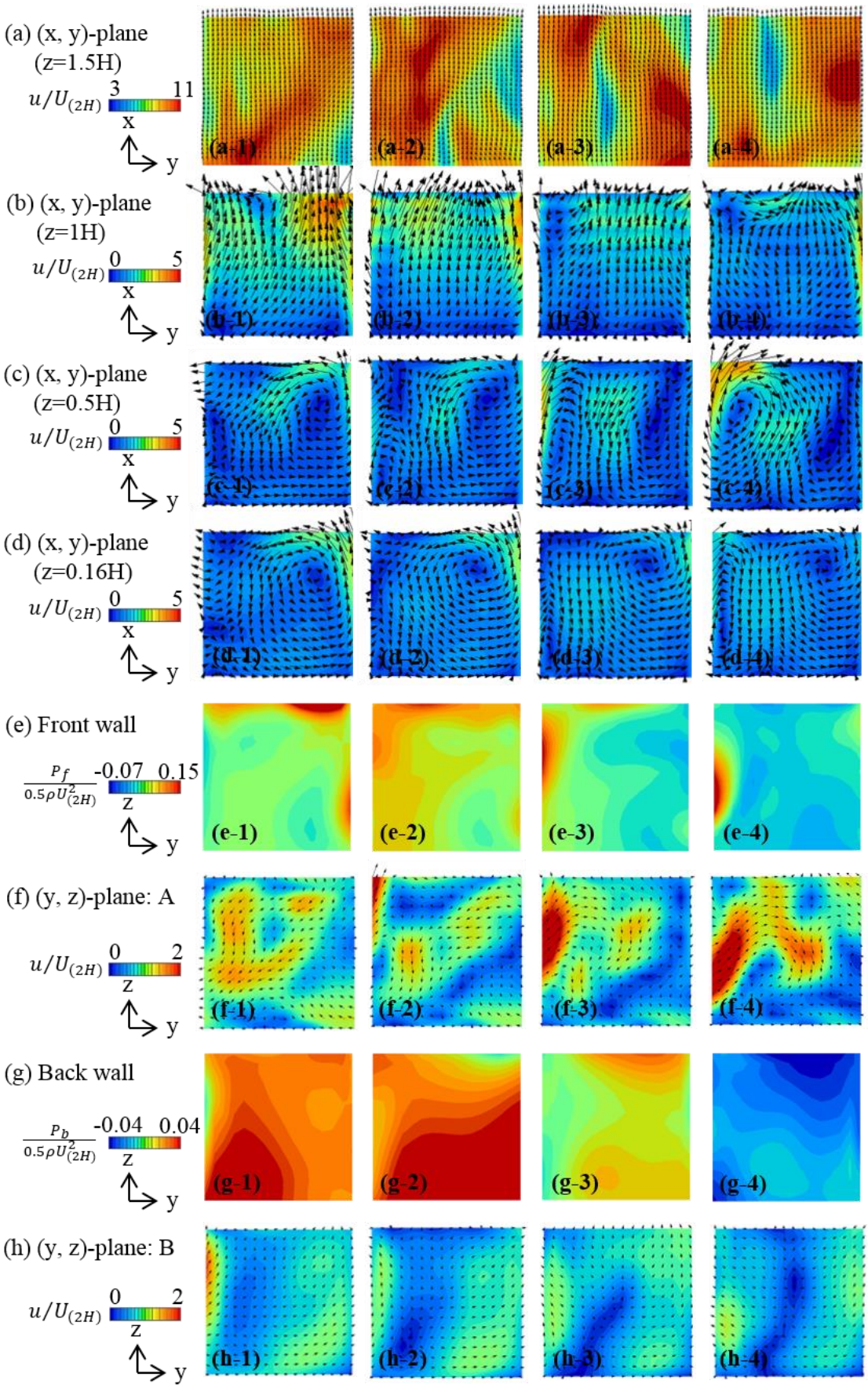

Fig. 6 Instantaneous distributions of velocity and pressure for SQ in planes shown in Fig. 5. The number indicates the sampling time: from 1 to 4 for 105s, 105.02s, 105.04s, and 105.06s, respectively.

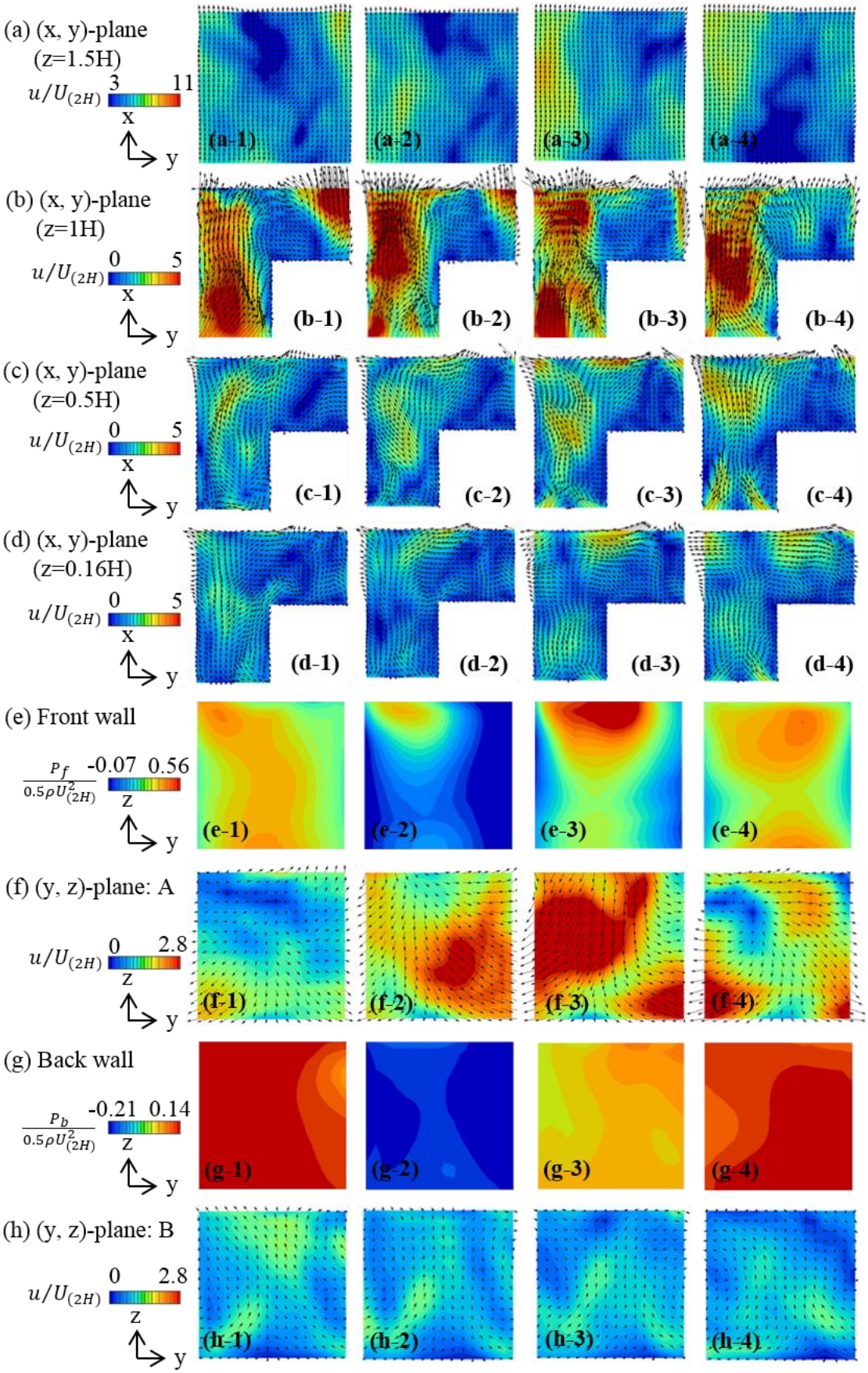

Fig. 7 Instantaneous distributions of velocity and pressure for ST in planes shown in Fig. 5. The number indicates the sampling time: from 1 to 4 for 105s, 105.02s, 105.04s, and 105.06s, respectively.

CONCLUSIONS

Large-eddy simulation was performed to investigate the instantaneous features of flow and wall-pressure acting on two differently arranged arrays of regular cubes.

Firstly, we demonstrated that for both arrays, the higher positions on cubes have greater ventilation efficiency compared to the lower levels. We then confirmed that the mean distributions of wall pressure are dominated by the widely reported mean flow structures around the cube arrays, such as skimming flow over the top of cubes, and reverse flow and convergent flow within the cavity, which are specific to the geometry of each cube array.

Secondly, the unsteady distributions of pressure and velocity fields are visualized by time-series snapshots. The instantaneous distribution of wall pressure is much different from the mean distribution. The results obtained for the limited sampling period imply that the differing instantaneous features of wall pressure distribution are due to the layout of the cube arrays.

ACKNOWLEDGEMENTS

This research was financially supported by JSPS KAKENHI Grant Number-25820282.

REFERENCES

Coceal, C., Thomas, T.G., Castro, I.P., Belcher, S.E. 2006. Mean flow and turbulence statistics over groups of urban-like cubical obstacles, Boundary-Layer Meteorology, Vol.121, pp.491-519

Haghighat, F., Rao, J., Fazio, P. 1991. The influence of turbulent wind on air change rates – a modelling approach, Building and Environment, Vol.26, No.2, pp.95-109

Jiang, Y., Chen, Q. 2001. Study of natural ventilation in buildings by large eddy simulation, Journal of Wind Engineering and Industrial Aerodynamics, Vol.89, pp.1155-1178

Kanda, M. 2006. Large-eddy simulations on the effects of surface geometry of building arrays on turbulent organized structures, Boundary-Layer Meteorology, Vol.118, pp.151-168

Marshall, R. 1975. A study of wind pressure on single-family dwelling in model and full scale, Journal of Industrial Aerodynamics, Vol.1, pp.177-199

Zaki, S.A., Hagishima, A., Tanimoto, J. 2012. Experimental study of wind-induced ventilation in urban building of cube arrays with various layouts, Journal of Wind Engineering and Industrial Aerodynamics, Vol.103, pp.31-40